How to cite: *Angew. Chem. Int. Ed.* **2023**, *62*, e202301969
doi.org/10.1002/anie.202301969

Proteomics

Digital Microfluidics and Magnetic Bead-Based Intact Proteoform Elution for Quantitative Top-down Nanoproteomics of Single *C. elegans* Nematodes

*Jan Leipert, Philipp T. Kaulich, Max K. Steinbach, Britta Steer, Konrad Winkels, Christine Blurton, Matthias Leippe, and Andreas Tholey**

Abstract: While most nanoproteomics approaches for the analysis of low-input samples are based on bottom-up proteomics workflows, top-down approaches enabling proteoform characterization are still underrepresented. Using mammalian cell proteomes, we established a facile one-pot sample preparation protocol based on protein aggregation on magnetic beads and intact proteoform elution using 40 % formic acid. Performed on a digital microfluidics device, the workflow enabled sensitive analyses of single *Caenorhabditis elegans* nematodes, thereby increasing the number of proteoform identifications compared to in-tube sample preparation by 46 %. Label-free quantification of single nematodes grown under different conditions allowed to identify changes in the abundance of proteoforms not distinguishable by bottom-up proteomics. The presented workflow will facilitate proteoform-directed analysis on samples of limited availability.

Recently technological advances and efforts for the miniaturization of sample preparation platforms have enabled nanoproteomics analyses with minute amounts of biological material.[1] Although considerable progress has been made, e.g., towards label-free proteomics of few or even single mammalian cells,[2–4] these efforts have largely been focused on bottom-up (BU) proteomics relying on the digestion of proteins into peptides followed by peptide level LC–MS analysis, and protein inference by means of bioinformatics methods. In top-down (TD) proteomics, proteins are not digested but analyzed at the intact level. Despite being technically more challenging, TD proteomics offers several advantages. In contrast to BU proteomics, TD approaches enable the identification of intact proteoforms,[5] thereby directly delivering information about posttranslational modifications, protein chain truncations, and about splice variants or isoforms.[6–8] However, TD protein analysis is inherently associated with markedly lower sensitivity.[9] Accordingly, conventional approaches still necessitate relatively large protein material input and specialized sample preparation workflows.[10] To date, TD nanoproteomics approaches have only sparsely been reported. TD sample preparation for low cell numbers based on the nanoPOTS workflow allowed the identification of up to 620 proteoforms from 770 HeLa cells and quantification of proteoforms from tissue sections.[11,12] More recently, single-cell TD proteomics employing on-capillary lysis followed by CE-MS/MS was presented.[13]

Single-pot, solid-phase-enhanced sample preparation (SP3),[14] a versatile one-pot sample preparation strategy, has recently been adapted for numerous sample types and applications in BU proteomics.[15] In SP3, proteomes are non-covalently captured by aggregation on paramagnetic beads, followed by a proteolytic digestion step on the beads releasing peptides into the supernatant. By efficiently depleting salts, detergents and other contaminant components through rinsing steps with organic solvent, SP3 is especially suited for low-input BU proteomics,[16] in particular in combination with digital microfluidics (DMF).[17,18]

The binding of intact proteins to SP3 beads is particularly stable and requires detergent mixtures for efficient protein recovery.[15] Despite efforts made towards SP3 intact protein elution with LC–MS compatible reagents for TD analysis,[19,20] to the best of our knowledge, a protocol enabling SP3 TD analysis of low protein-input samples has not been reported so far, in particular not in combination with DMF.

Aiming to develop a highly sensitive TD nanoproteomics sample preparation method, we tested SP3 intact protein elution with reagents compatible with nano LC–MS. Lysates of Jurkat T cells were mixed with SP3 beads and organic solvents to initiate protein-bead aggregation. Next, proteins were eluted off the beads by addition of candidate reagents (LC–MS compatible detergents or volatile chemicals, Table S1). Elution completeness was validated by proteolytic

[*] J. Leipert, P. T. Kaulich, M. K. Steinbach, B. Steer, K. Winkels, Dr. A. Tholey
Systematic Proteome Research & Bioanalytics, Institute for Experimental Medicine, Christian-Albrechts-Universität zu Kiel
24105 Kiel (Germany)
E-mail: a.tholey@iem.uni-kiel.de

C. Blurton, Dr. M. Leippe
Comparative Immunobiology, Zoological Institute, Christian-Albrechts-Universität zu Kiel
24118 Kiel (Germany)

© 2023 The Authors. Angewandte Chemie International Edition published by Wiley-VCH GmbH. This is an open access article under the terms of the Creative Commons Attribution Non-Commercial License, which permits use, distribution and reproduction in any medium, provided the original work is properly cited and is not used for commercial purposes.

 © 2023 The Authors. Angewandte Chemie International Edition published by Wiley-VCH GmbH

digestion of non-eluted proteins and subsequent LC–MS analysis. As negative and positive controls for elution, water (no elution) and the anionic detergent SDS (complete elution) were used (Figure 1A and Figure S1A). First, we tested the nonionic detergent dodecyl maltoside (DDM), which was previously employed for the TD LC–MS analysis of few cells.[11] However, this detergent showed no resolubilization of proteins aggregated on SP3 beads (Figure S1B). Similarly, the fluorinated solvent hexafluoroisopropanol, which has been employed for intact protein extraction,[21] was inefficient for intact protein elution (Figure S1C).

A common method to solubilize proteins is the use of cleavable, LC–MS compatible detergents, e.g., the acid-cleavable anionic surfactant RapiGest (RG). Having similar solubilization properties as SDS, RG was successfully used to elute proteins from SP3 beads (Figure S1D). However, follow-up acidification resulted in co-precipitation of proteins and insoluble RG cleavage products,[22] an effect we also observed for BU low-input samples.[17]

Previously, Dagley et al. demonstrated TD-SP3 elution by means of concentrated (80 %) formic acid (FA).[19] To prevent protein formylation, elution was carried out at −20 °C. Although our BU approach corroborated this mechanism (Figure S1E), subsequent ten-fold dilution of FA eluates prior to LC–MS analysis leads to large volumes (300 µL in the original protocol) unfavorable for low protein input proteomics. We therefore tested a FA concentration decreased to 40 % and observed an elution efficiency comparable both to 80 % FA and the SDS control (Figure 1B).

Having identified an effective method for SP3 protein elution, we set out to translate this method to the TD analysis of nanoproteomics samples. To boost sensitivity, we employed high-field asymmetric-waveform ion mobility spectrometry (FAIMS) and internal compensation voltage (CV) stepping previously developed for conventional TD proteomics.[23] Similar to low-input or even single-cell BU studies,[2] TD nanoproteomics considerably benefits from front end ion fractionation, as we could show by TD analysis of dilute preparations (1 000 cell equivalents) of Jurkat T cell proteins with and without FAIMS (Figure 1C and Figure S2A). Proteoform identifications were increased over the entire mass range when using FAIMS, covering almost all proteoforms found without gas-phase fractionation (Figure S2B and C).

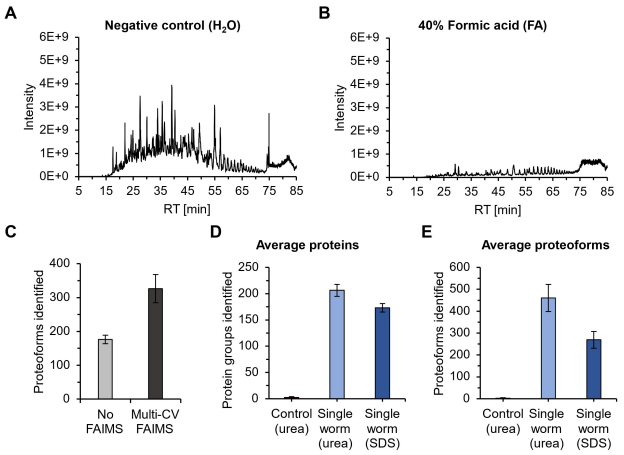

Figure 1. Elution of intact proteins aggregated on magnetic beads. Total ion chromatogram of digest of Jurkat T cell proteins, which remained on SP3 beads after elution with A) deionized water or B) chilled FA (−20 °C, 40 %). C) Proteoforms identified after SP3 elution (40 % FA) of proteins from Jurkat T cells analyzed by LC–MS/MS or LC-FAIMS-MS/MS. Injected amounts correspond to approximately 1000 cells; $n = 4$. D) Average protein groups and E) proteoforms identified from blank samples or single *C. elegans* nematodes lysed with urea or SDS buffer using SP3 elution (40 % FA) in-PCR tube sample preparation and LC-FAIMS-MS/MS analysis; $n = 3$, error bars: standard deviations.

Tissue samples and small animals (or parts thereof) are important targets for nanoproteomics.[24,25] The nematode *Caenorhabditis elegans* (*C. elegans)* has been employed as a model organism for groundbreaking discoveries in developmental and basic cell biology.[26] Conventional proteome studies of *C. elegans* are usually performed with several thousands of worms masking the biological state of single individuals. For example, individual specimens have been shown to react differently to environmental stimuli.[27] Accordingly, by characterization of individuals at the proteoform level, possibly in conjunction with investigations of morphology, behavior, and epigenetics, the heterogeneity within a population could be studied. To this end, robust sample preparation methods are required. However, we recently found that the worm cuticle cannot be disintegrated by mild, MS compatible detergents.[25] Also, direct one-pot treatment with acid buffers may result in residual debris, which may lead to problems such as column clogging in the downstream LC–MS analysis. To test the suitability of the FA-based TD-SP3 intact protein elution, we disrupted single adult nematodes, which consist of an invariant number of 959 somatic cells, in PCR-tubes with lysis cocktails containing urea/NP-40 surfactant or SDS detergent, followed by SP3 clean-up (Figure 1D and E). Elution of the bead-aggregated proteome samples with chilled (−20 °C) formic acid (40 %) and TD LC–MS/MS analysis of the complete sample on an Orbitrap Fusion Lumos Tribrid MS identified 269 ± 39 ($n = 3$, SDS) and 461 ± 62 (urea) proteoforms (deriving from 173 ± 8 and 206 ± 12 protein groups, respectively) from single nematodes (Figure S3). Notably, we also found no significant formylation of proteins eluted with 40 % FA (Figure S4A and B).

Downscaling of the SP3 procedure is limited by manual pipetting, requiring volumes in the range of 3–10 µL to ensure reproducible bead handling and analytical results.[15] However, the reduction of processed volumes is generally considered a sensitivity-determining factor in nanoproteomics.[1] To further miniaturize TD-SP3, we tested the methodology on a DMF liquid handling device.[28] This lab-on-a-chip technology enables a digitally controlled manipulation of solvent droplets on an array of insulated and hydrophobically coated electrodes (Figure 2 and Figure S5).

With a driving electrowetting force generated by voltage application to selected electrodes, nano- to microliter-sized droplets can be moved, split, or merged.[29,31] We have

© 2023 The Authors. Angewandte Chemie International Edition published by Wiley-VCH GmbH

15213773, 2023, 28, Downloaded from https://onlinelibrary.wiley.com/doi/10.1002/anie.202301969 by Christian-Albrechts-Universitat, Wiley Online Library on [22/01/2025]. See the Terms and Conditions (https://onlinelibrary.wiley.com/terms-and-conditions) on Wiley Online Library for rules of use; OA articles are governed by the applicable Creative Commons License

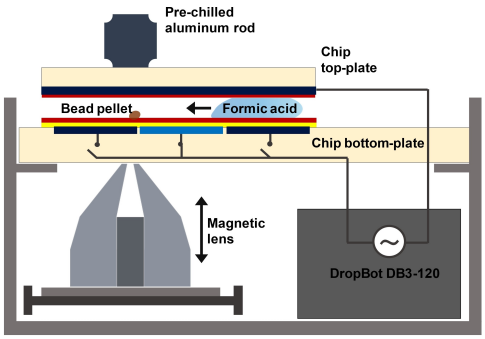

Figure 2. Digital microfluidics setup used for TD-SP3 elution of intact proteins illustrating a chip device composed of a bottom-plate with patterned electrodes, onto which an insulating dielectric (yellow) and a hydrophobic (red) coating is applied.[29,30] Droplets (e.g. samples, lysis buffers, formic acid) are displaced by connecting the driving voltage to an adjacent electrode with the top-plate set to ground. To pellet SP3 magnetic beads, a magnetic lens is used. When formic acid is moved across the chip, the top-plate is passively cooled with an aluminum rod.

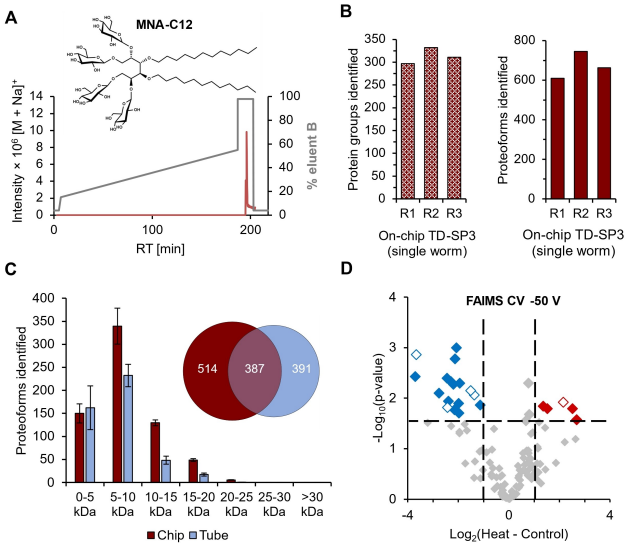

Figure 3. Analysis of single *C. elegans* nematodes using an LC–MS compatible detergent and DMF-SP3. A) Extracted ion chromatogram of the nonionic detergent MNA-C12 in a protein sample shows late elution from a C_4-RP column. B) Number of protein groups and proteoforms identified from single adult nematodes using TD-DMF-SP3 sample preparation in three replicates. C) Proteoform mass distributions and overlap of unique proteoforms (inset) of analyses of single adult nematodes lysed on-chip or in-tube using urea buffer. D) Heat-induced proteome changes based on the label-free quantification of proteoforms from single L4-stage nematodes extracted on-chip (FAIMS CV subset of −50 V). Blue and red diamonds: proteoforms with significant differential abundances; open symbols: proteoforms of 40S ribosomal protein S28.

previously integrated the handling of SP3 magnetic beads on a readily available commercial DMF system,[30] thereby achieving higher sensitivity and improved quantification accuracy in low-input BU proteome analyses as compared to an in-tube SP3 procedure.[17,18,25] While SP3-aggregated proteins are effectively eluted by FA, DMF requires the incorporation of a passivating detergent to maintain mobility of protein-containing droplets. Long-alkyl chain, nonionic maltoside detergents have been used for low-input proteomics[2] and also DMF applications,[18] as they elute sufficiently late from C_{18}-RP stationary phases for compatibility with BU analyses. Here, we monitored retention of eight different detergents on a C_4-RP nano-LC column (Figure S6, Table S2, and Supporting Information Discussion). Nonionic DDM eluted during the gradient run, possibly interfering with proteoform detection. In contrast, perGlu-bisdodecyl mannitol (MNA-C12), a novel mannitol-based amphiphile,[32] eluted only during the post-gradient wash step with high organic solvent content (Figure S6 and Figure 3A). As this nonionic detergent also led to reasonable droplet mobility on DMF, we based our miniaturized TD nanoproteomics strategy on DMF-SP3 sample clean-up, 40 % FA protein elution, and subsequent dilution with aqueous MNA-C12 solution.

As input samples, droplets containing single adult *C. elegans* specimens were loaded on a DMF chip. Each nematode was subsequently lysed by merging with a droplet of urea/NP-40 lysis buffer (combined volume: 2 µL). Extracted proteins were reduced by dithiothreitol in the buffer during the same step and aggregated on SP3 magnetic beads. SP3 binding and rinsing steps were performed by means of a magnetic lens installed below the chip substrate as described previously (Figure 2).[18,33] For proteoform elution, bead pellets were immersed in droplets of 40 % FA (−20 °C) and incubated for 15 min. Passive cooling was applied prior transfer of the chip to a freezer cabinet and effectively prevented formylation during FA elution (Figure S4C).[19] Protein eluates were separated from the SP3 beads, diluted with droplets of MNA-C12 (0.01 % wt/vol), and aspirated from the chip.[17] Analysis of single worms prepared by TD-DMF-SP3 allowed the identification of 673 ± 69 ($n = 3$) proteoforms, corresponding to an average of 313 ± 18 protein groups (Figure 3B). Remarkably, compared to the in-tube urea preparations (461 ± 62), on-chip TD-SP3 led to a 46 % increase of proteoform identifications (Figure 3C).

We next tested the developed TD workflow for performing label-free quantification (LFQ). Single nematodes were picked from two distinct populations of L4 larvae, one of which was subjected to heat-stress (33 °C), while the other worm population was kept at 20 °C (control).[25] Individual worms ($n = 4$ per condition) were lysed on-chip and proteins were extracted using the TD- DMF-SP3 method. After LC-FAIMS-MS/MS analysis, the resulting data files were sliced into subsets filtered by the applied CVs, with the quantification for each of these performed separately (Figure 3D, Figure S7, and Supporting Information Discussion).[34] In total, 34 proteoforms showed differential abundances ($\log_2$ ±1 cut-off) between the heat-stressed worms and the control group (Table S3).

Factors hampering LFQ of intact proteoforms in nanoproteomics samples are the limited number of identified proteoforms and the high rate of missing values. Due to the latter and the strict filtering (leading to the removal of

© 2023 The Authors. Angewandte Chemie International Edition published by Wiley-VCH GmbH

15213773, 2023, 28, Downloaded from https://onlinelibrary.wiley.com/doi/10.1002/anie.202301969 by Christian-Albrechts-Universitat, Wiley Online Library on [22/01/2025]. See the Terms and Conditions (https://onlinelibrary.wiley.com/terms-and-conditions) on Wiley Online Library for rules of use; OA articles are governed by the applicable Creative Commons License

≈50 % of the initial data points; Table S4), several proteoforms could not be quantified. For example, proteoforms assigned to four different heat-shock proteins were found exclusively in the heat-stress group (Table S5), confirming earlier BU proteomics data.[25]

The majority of proteoforms decreased in abundance in the heat-group were ribosomal proteins. Five (out of 18 identified) proteoforms assigned to the 40S ribosomal protein S28 were differentially abundant (Figure 3D). Of these five, four N- and C-terminally truncated proteoforms were of higher abundance in the control, while the fifth proteoform, corresponding to the N-terminally acetylated canonical sequence of the 40S ribosomal protein S28, was more abundant in heat-treated worms (Figure S8, Figure 3D). This protein was also identified in a previously performed single worm BU proteomics analysis on a DMF-SP3 platform.[25] However, due to the peptide-based analysis and by inferring only a single encoded protein from the identified peptides, the information about the different proteoforms was lost (Figure S9). Moreover, due to shared peptides from different proteoforms with opposite abundance changes, the BU proteomics-based quantification revealed overall no effect on the abundance of the inferred protein. This again highlights the great benefit of TD proteomics, allowing to distinguish and also quantify different proteoforms of the same protein with potentially different biological functions.

We here developed a readily accessible low-input TD proteomics sample preparation workflow, which combines SP3 with a low-cost DMF liquid handling system. The workflow proved to be highly sensitive, quantifying changes in proteoform abundances of individual model organisms with less than 1000 cells. Further optimization of the approach will be possible, e.g., by a considerable reduction of the processed volumes using down-scaled DMF electrodes,[35] modified lysis conditions, and improved proteoform separation. Notably, with the development and availability of larger electrode arrays,[36] we envision automated, higher throughout TD nanoproteomics enabled by DMF-SP3. The developed protocol also holds potential for TD proteomics of few, or even single mammalian cells to study cell type-specific differences in proteome composition at proteoform level.

Acknowledgements

This work was funded by the Deutsche Forschungsgemeinschaft, Cluster of Excellence "Precision Medicine in Inflammation, RTF-V", and the SFB 1182/Z3. Open Access funding enabled and organized by Projekt DEAL.

Conflict of Interest

The authors declare no conflict of interest.

Data Availability Statement

The data that support the findings of this study are openly available in Pride/ProteomeXchange at https://www.ebi.ac.uk/pride/, reference number PXD39883.

Keywords: Ion Mobility · Mass Spectrometry · Microfluidics · Proteoforms · Proteomics

[1] Y. Zhu, P. D. Piehowski, R. T. Kelly, W.-J. Qian, *Expert Rev. Proteomics* **2018**, *15*, 865–871.
[2] Y. Cong, K. Motamedchaboki, S. A. Misal, Y. Liang, A. J. Guise, T. Truong, R. Huguet, E. D. Plowey, Y. Zhu, D. Lopez-Ferrer, R. T. Kelly, *Chem. Sci.* **2021**, *12*, 1001–1006.
[3] B. Budnik, E. Levy, G. Harmange, N. Slavov, *GenomeBiology* **2018**, *19*, 161.
[4] C. Lombard-Banek, S. A. Moody, P. Nemes, *Angew. Chem. Int. Ed.* **2016**, *55*, 2454–2458.
[5] L. M. Smith, N. L. Kelleher, *Nat. Methods* **2013**, *10*, 186–187.
[6] R. D. Melani, V. R. Gerbasi, L. C. Anderson, J. W. Sikora, T. K. Toby, J. E. Hutton, D. S. Butcher, F. Negrão, H. S. Seckler, K. Srzentić, L. Fornelli, J. M. Camarillo, R. D. LeDuc, A. J. Cesnik, E. Lundberg, J. B. Greer, R. T. Fellers, M. T. Robey, C. J. DeHart, E. Forte, C. L. Hendrickson, S. E. Abbatiello, P. M. Thomas, A. I. Kokaji, J. Levitsky, N. L. Kelleher, *Science* **2022**, *375*, 411–418.
[7] E. N. McCool, T. Xu, W. Chen, N. C. Beller, S. M. Nolan, A. B. Hummon, X. Liu, L. Sun, *Sci. Adv.* **2022**, *8*, eabq6348.
[8] L. M. Smith, J. N. Agar, J. Chamot-Rooke, P. O. Danis, Y. Ge, J. A. Loo, L. Paša-Tolić, Y. O. Tsybin, N. L. Kelleher, Consortium for Top-Down Proteomics, *Sci. Adv.* **2021**, *7*, eabk0734.
[9] L. V. Schaffer, R. J. Millikin, R. M. Miller, L. C. Anderson, R. T. Fellers, Y. Ge, N. L. Kelleher, R. D. LeDuc, X. Liu, S. H. Payne, L. Sun, P. M. Thomas, T. Tucholski, Z. Wang, S. Wu, Z. Wu, D. Yu, M. R. Shortreed, L. M. Smith, *Proteomics* **2019**, *19*, 1800361.
[10] T. K. Toby, L. Fornelli, N. L. Kelleher, *Annu. Rev. Anal. Chem.* **2016**, *9*, 499–519.
[11] M. Zhou, N. Uwugiaren, S. M. Williams, R. J. Moore, R. Zhao, D. Goodlett, I. Dapic, L. Paša-Tolić, Y. Zhu, *Anal. Chem.* **2020**, *92*, 7087–7095.
[12] Y.-C. Liao, J. M. Fulcher, D. J. Degnan, S. M. Williams, L. M. Bramer, D. Veličković, K. J. Zemaitis, M. Veličković, R. Sontag, R. J. Moore, *Mol. Cell. Proteomics* **2023**, *22*, 100491.
[13] K. R. Johnson, Y. Gao, M. Greguš, A. R. Ivanov, *Anal. Chem.* **2022**, *94*, 14358–14367.
[14] C. S. Hughes, S. Foehr, D. A. Garfield, E. E. Furlong, L. M. Steinmetz, J. Krijgsveld, *Mol. Syst. Biol.* **2014**, *10*, 757.
[15] C. S. Hughes, S. Moggridge, T. Müller, P. H. Sorensen, G. B. Morin, J. Krijgsveld, *Nat. Protoc.* **2019**, *14*, 68–85.
[16] Z. Yang, Z. Zhang, D. Chen, T. Xu, Y. Wang, L. Sun, *Anal. Chem.* **2021**, *93*, 10568–10576.
[17] J. Leipert, A. Tholey, *Lab Chip* **2019**, *19*, 3490–3498.
[18] J. Leipert, M. K. Steinbach, A. Tholey, *Anal. Chem.* **2021**, *93*, 6278–6286.
[19] L. F. Dagley, G. Infusini, R. H. Larsen, J. J. Sandow, A. I. Webb, *J. Proteome Res.* **2019**, *18*, 2915–2924.
[20] Z. Yang, X. Shen, D. Chen, L. Sun, *J. Proteome Res.* **2020**, *19*, 3315–3325.
[21] J. Franck, R. Longuespee, M. Wisztorski, A. V. Remoortere, R. V. Zeijl, A. Deelder, M. Salzet, L. McDonnell, I. Fournier, *Med. Sci. Monit.* **2010**, *16*, BR293–BR299.

© 2023 The Authors. Angewandte Chemie International Edition published by Wiley-VCH GmbH

15213773, 2023, 28, Downloaded from https://onlinelibrary.wiley.com/doi/10.1002/anie.202301969 by Christian-Albrechts-Universitat, Wiley Online Library on [22/01/2025]. See the Terms and Conditions (https://onlinelibrary.wiley.com/terms-and-conditions) on Wiley Online Library for rules of use; OA articles are governed by the applicable Creative Commons License

[22] K. A. Brown, B. Chen, T. M. Guardado-Alvarez, Z. Lin, L. Hwang, S. Ayaz-Guner, S. Jin, Y. Ge, *Nat. Methods* **2019**, *16*, 417–420.
[23] P. T. Kaulich, L. Cassidy, K. Winkels, A. Tholey, *Anal. Chem.* **2022**, *94*, 3600–3607.
[24] A. M. do Canto, A. S. Vieira, A. H. B. Matos, B. S. Carvalho, B. Henning, B. A. Norwood, S. Bauer, F. Rosenow, R. Gilioli, F. Cendes, I. Lopes-Cendes, *Sci. Rep.* **2020**, *10*, 4412.
[25] M. K. Steinbach, J. Leipert, C. Blurton, M. Leippe, A. Tholey, *J. Proteome Res.* **2022**, *21*, 1986–1996.
[26] M. Markaki, N. Tavernarakis, *Biotechnol. J.* **2010**, *5*, 1261–1276.
[27] S. L. Rea, D. Wu, J. R. Cypser, J. W. Vaupel, T. E. Johnson, *Nat. Genet.* **2005**, *37*, 894–898.
[28] J. Lamanna, E. Y. Scott, H. S. Edwards, M. D. Chamberlain, M. D. M. Dryden, J. Peng, B. Mair, A. Lee, C. Chan, A. A. Sklavounos, A. Heffernan, F. Abbas, C. Lam, M. E. Olson, J. Moffat, A. R. Wheeler, *Nat. Commun.* **2020**, *11*, 5632.
[29] K. Choi, A. H. C. Ng, R. Fobel, A. R. Wheeler, *Annu. Rev. Anal. Chem.* **2012**, *5*, 413–440.
[30] R. Fobel, C. Fobel, A. R. Wheeler, *Appl. Phys. Lett.* **2013**, *102*, 193513.
[31] J. Peng, C. Chan, S. Zhang, A. A. Sklavounos, M. E. Olson, E. Y. Scott, Y. Hu, V. Rajesh, B. B. Li, M. Dean Chamberlain, S. Zhang, H. Peng, A. R. Wheeler, *Chem. Sci.* **2023**, *14*, 2887–2900.
[32] H. Hussain, Y. Du, N. J. Scull, J. S. Mortensen, J. Tarrasch, H. E. Bae, C. J. Loland, B. Byrne, B. K. Kobilka, P. S. Chae, *Chem. Eur. J.* **2016**, *22*, 7068–7073.
[33] K. Choi, A. H. C. Ng, R. Fobel, D. A. Chang-Yen, L. E. Yarnell, E. L. Pearson, C. M. Oleksak, A. T. Fischer, R. P. Luoma, J. M. Robinson, J. Audet, A. R. Wheeler, *Anal. Chem.* **2013**, *85*, 9638–9646.
[34] T. Xu, X. Shen, Z. Yang, D. Chen, R. A. Lubeckyj, E. N. McCool, L. Sun, *Anal. Chem.* **2020**, *92*, 15890–15898.
[35] E. R. F. Welch, Y.-Y. Lin, A. Madison, R. B. Fair, *Biotechnol. J.* **2011**, *6*, 165–176.
[36] J. Li, C.-J. "CJ" Kim, *Lab Chip* **2020**, *20*, 1705–1712.

Manuscript received: February 8, 2023
Accepted manuscript online: April 17, 2023
Version of record online: May 31, 2023

© 2023 The Authors. Angewandte Chemie International Edition published by Wiley-VCH GmbH

15213773, 2023, 28, Downloaded from https://onlinelibrary.wiley.com/doi/10.1002/anie.202301969 by Christian-Albrechts-Universitat, Wiley Online Library on [22/01/2025]. See the Terms and Conditions (https://onlinelibrary.wiley.com/terms-and-conditions) on Wiley Online Library for rules of use; OA articles are governed by the applicable Creative Commons License